



NICOTINAMIDE, ACETATE AND THEIR TWO NEW COMPLEXES WITH Zn(II) AND Cd(II)

Laurențiu PRICOP,^{a,*} Maria Olimpia MICLĂUȘ,^b Mihaela Elena BADEA,^a Ana Maria HANGANU^{c,a} and Mihaela GANCIAROV^d

^aDepartment of Inorganic Chemistry, Organic Chemistry, Biochemistry and Catalysis, Faculty of Chemistry, University of Bucharest, 90 – 92 Panduri St., 050663, Bucharest, Roumania; e-mail: laurp2002@yahoo.com, e_m_badea@yahoo.com

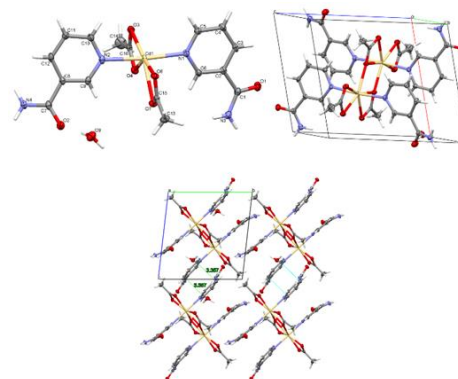
^bNational Institute for Research and Development of Isotopic and Molecular Technologies, 67-103 Donat St., 400293, Cluj-Napoca, Roumania; e-mail: maria.miclaus@itim-cj.ro

^c"C. D. Nenitescu" Institute of Organic and Supramolecular Chemistry of the Roumanian Academy, Spl. Independenței 202B, 060023, Bucharest, Roumania; e-mail: anamaria.hanganu@unibuc.ro

^dAnalysis Team, National Institute for Research & Development in Chemistry and Petrochemistry—ICECHIM, Splaiul Independenței No. 202, Sector 6, 060021 Bucharest, Roumania; e-mail: mihaela.ganciarov@icechim.ro

Received December 10, 2023

Two new complexes of Zn(II) and Cd(II) with acetate and nicotinamide as mixed ligands were synthesized and characterized. The Zn(II) complex is mononuclear, $[\text{Zn}(\text{ac})_2(\text{NA})_2]$ (**1**), while the Cd(II) is a dinuclear one, $[\text{Cd}_2(\text{ac})_4(\text{NA})_4] \cdot 2\text{H}_2\text{O}$ (**2**), where ac = acetate and NA = nicotinamide. The compounds were characterized by means of single-crystal X-ray diffraction, FTIR, ^1H NMR, ^{13}C NMR spectroscopy, thermal analysis and elemental analysis. The geometry of the metal ion is distorted tetrahedral for Zn(II) and distorted pentagonal bipyramid geometry for Cd(II). In the dinuclear complex, each metal ion is coordinated by three acetate groups, but there are two different types of coordination modes for the acetate ligands: bidentate chelating and bridging bidentate chelating.



INTRODUCTION

Zinc is an essential microelement for the human body, with a well defined role in the functioning of the proteins, as well as in the metabolism of the nucleic acids. Many hundreds of enzymes contain this element, carbonic anhydrase being one of them, the first zinc enzyme discovered in 1940.¹ Some of the

enzymes contain three zinc ions, like phosphatases, while others have binuclear zinc complexes in their active centers, like aminopeptidases.² Certain Zn(II) complexes have strong action as anti-diabetic compounds^{3,4} and a more powerful antihypertensive effect than the corresponding metal-free drugs.⁵ Also, zinc coordination compounds have antioxidant activity,⁶ antibacterial and antifungal properties.^{7,8}

* Corresponding author: laurp2002@yahoo.com

Unlike zinc, cadmium is a very toxic element, known for its harmful action on the renal tubes, which causes osteomalacia associated with severe bone pain, *i.e.* Itai-itai disease.⁹ Cd(II) complexes with bipyridine or bipyridine derivatives and acetate as mixed ligands show a marked antibacterial activity,^{10,11} cadmium acetate being more toxic than the coordination compounds.¹² Also, two complexes of Cd(II) with nicotinamide were proved to have a powerful antimicrobial and antifungal action.¹³

A study was focused on the toxic effects of Zn(II) and Cd(II) complexes with acetate and nicotinamide as ligands on some photosynthesizing organisms. The dry mass of the contaminated plants was lower than that of the control plants and the metals were accumulated mainly in the roots. Nevertheless, both complexes were not characterized by means of single crystal X-ray diffraction.¹⁴ On the same note, another research studied the effect of some Cd(II) complexes with nicotinamide, including the acetate one, on microalgae growth. The conclusion was that nicotinamide diminished the toxic effect of cadmium on algal growth and chlorophyll production.¹⁵

On the other hand, acetate is a well-known ligand for its versatility and can coordinate to the metal ions in several ways. In a single trinuclear complex of Zn(II), acetato ligands act in a monodentate, bridging monodentate and bridging bidentate manner.¹⁶ This variety of acetato coordination modes, the use of zinc acetate in the

treatment of Wilson's disease¹⁷ as well as the biological action of cadmium complexes with acetate and various pyridinic ligands, prompted us to synthesize and characterize new complexes with acetate and nicotinamide as mixed ligand. Very recently, we find out that a quite similar complex of Cd(II) was isolated and characterized.¹⁸

RESULTS

[Zn(ac)₂(NA)₂]

IR(ATR, cm⁻¹): ν_{as} (N-H), 3419 m; ν_s (N-H), 3291 m; ν_s (N-H), 3210 m; ν (C=O), 1703 s; ν (C=O), 1671 s; ν (C=N) + δ (N-H), 1600 s; ν_{as} (COO⁻), 1573 vs; ν (C-C), 1396 s; ν_s (COO⁻), 1382 vs; ν (C-N), 1325 s; ν (C-NH₂), 1209 m; ν (C-N), 1150 w; δ (C-H), 1110 w; δ (C-H) + ν (C-C), 1056 w; ρ_r (CH₃), 1027 w; ν (C-C), 928 w; γ (C-H), 836 w; γ (C-H), 804 w; ρ_w (NH₂), 700 s; ρ_w (NH₂), 679 s; δ (OCO), 652 m; β (C=O) + δ (N-H), 617 s; δ (C-NH₂) + γ (C=O) 517 m; ν (Zn - O), 434 m.

¹H-NMR (500 MHz, DMSO-d₆, δ ppm, J Hz): 9.08 (s, 2H, NH₂), 8.76 (s, 2H, NH₂), 8.24 (d, 2H, H-5, 7.8 Hz), 8.19 (s, 2H, H-1), 7.63 (m, 2H, H-3), 7.55 (m, 2H, H-4), 1.85 (s, 6H, CH₃) ppm.

¹³C-NMR (125 MHz, DMSO-d₆, δ ppm): 178.3, 166.7, 152.2, 149.1, 135.9, 130.2, 123.9, 22.2 ppm.

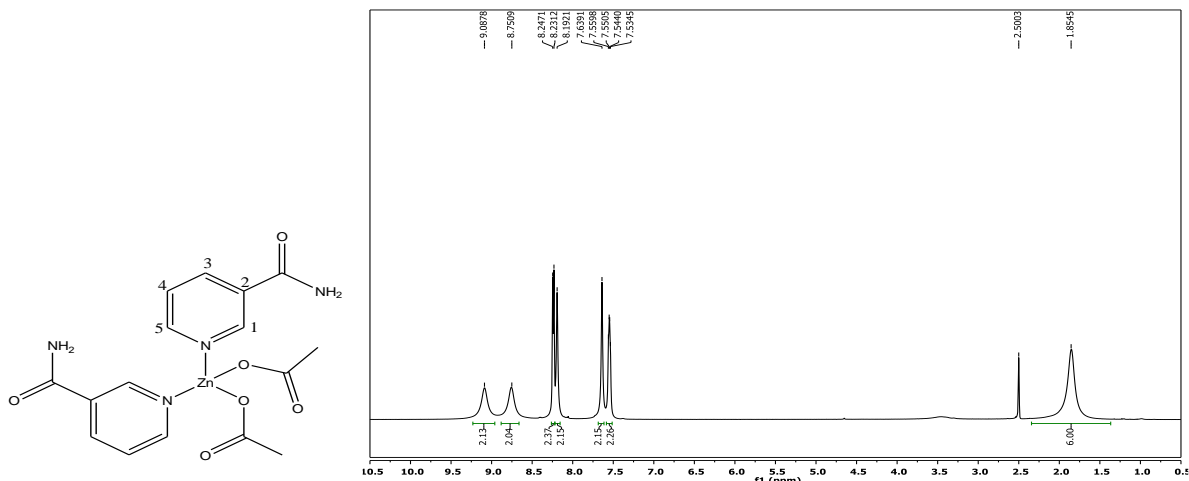


Fig. 1 – ¹H-NMR spectrum of the compound [Zn(ac)₂(NA)₂].

[Cd₂(ac)₄(NA)₄].2H₂O

IR(ATR, cm⁻¹): ν (O-H), 3536 sh; ν_{as} (N-H), 3352 m; ν_s (N-H), 3176 m; ν (C-H), 2990 w; ν (C=O), 1697 m; ν (C=O), 1673 s; ν (C=N), 1623 s; δ (N-H), 1597 s; ν_{as} (COO⁻), 1556 s; ν_s (COO⁻) + ν (C-C), 1392 s; ν_s (COO⁻), 1385 vs; ν (C-N), 1341

s; ν (C-NH₂), 1197 m; δ (C-H), 1125 w; δ (C-H) + ν (C-C), 1043 w; ρ_r (CH₃), 1029 w; ν (C-C), 934 w; γ (C-H), 832 w; γ (C-H), 781 w; ρ_w (NH₂), 693 s; ρ_w (NH₂), 671 s; δ (OCO), 646 s; β (C=O) + δ (N-H), 622 vs; δ (C-NH₂) + γ (C=O) 508 m; ν (Cd - O), 427 m.

¹H-NMR (500 MHz, DMSO-*d*₆, δ ppm, J Hz): 9.02 (d, 4H, H-1, 1.8 Hz), 8.70 (dd, 4H, H-5, 1.3 Hz, 4.8 Hz), 8.21 (dt, 4H, H-3, 1.8 Hz, 7.9 Hz), 8.17 (s, 4H, NH₂), 7.60 (s, 4H,

NH₂), 7.50 (dd, 4H, H-4, 4.8 Hz, 7.9 Hz), 1.83 (s, 12H, CH₃) ppm.

¹³C-NMR (125 MHz, DMSO-*d*₆, δ ppm): 177.9, 166.4, 152.0, 148.8, 135.4, 129.8, 123.5, 21.8 ppm.

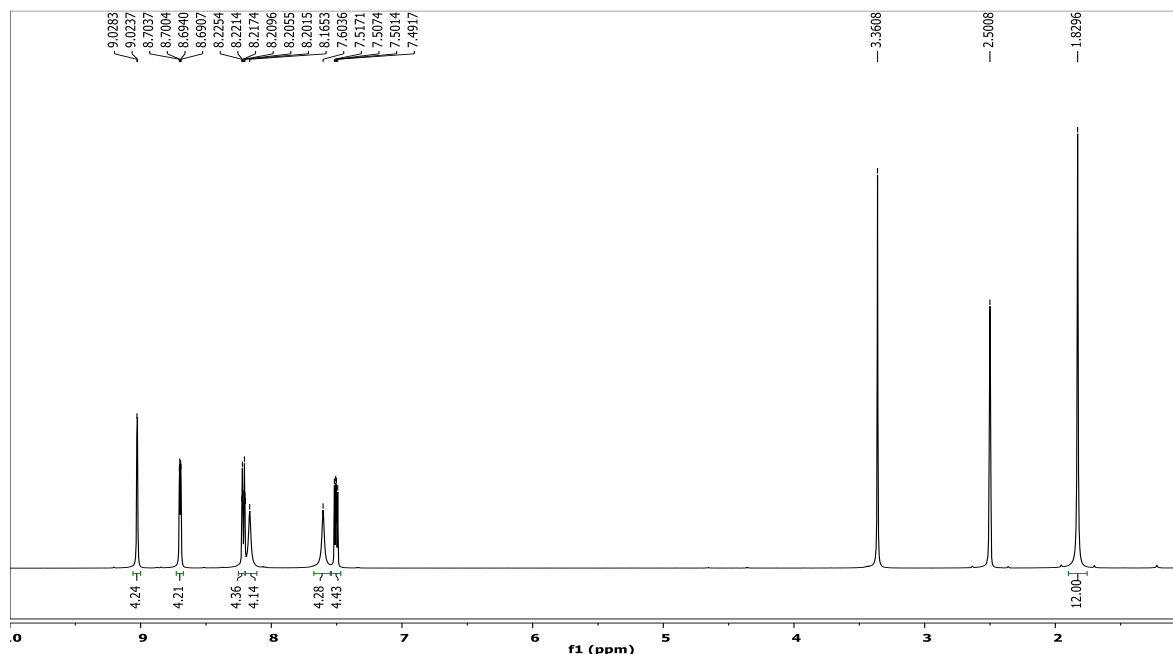


Fig. 2 – ¹H-NMR spectrum of the compound [Cd₂(ac)₄(NA)₄].2H₂O.

Table 1

Crystal data and structure refinement for complex (1) and complex (2)

| Identification code | (1) | (2) |
|---|--|---|
| Empirical formula | C ₁₆ H ₁₈ N ₄ O ₆ Zn | C ₁₆ H ₂₀ CdN ₄ O ₇ |
| Formula weight | 427.71 | 492.76 |
| Temperature/K | 149(40) | 124(2) |
| Crystal system | Triclinic | Triclinic |
| Space group | P-1 | P-1 |
| a/Å | 8.6393(10) | 9.3776(7) |
| b/Å | 10.7205(10) | 10.1013(6) |
| c/Å | 11.4017(8) | 10.6123(6) |
| α/° | 104.467(7) | 93.969(5) |
| β/° | 110.476(9) | 103.904(5) |
| γ/° | 99.313(9) | 99.906(5) |
| Volume/Å ³ | 921.05(16) | 954.81(11) |
| Z | 2 | 2 |
| ρ _{calc} g/cm ³ | 1.542 | 1.714 |
| μ/mm ⁻¹ | 1.374 | 1.190 |
| F(000) | 440.0 | 496.0 |
| Crystal size/mm ³ | 0.3 × 0.2 × 0.05 | 0.15 × 0.1 × 0.08 |
| Radiation | MoKα (λ = 0.71073) | MoKα (λ = 0.71073) |
| 2θ range for data collection/° | 5.686 to 58.138 | 6.72 to 57.628 |
| Index ranges | -10 ≤ h ≤ 11, -14 ≤ k ≤ 11, -15 ≤ l ≤ 15 | -11 ≤ h ≤ 12, -13 ≤ k ≤ 13, -11 ≤ l ≤ 14 |
| Reflections collected | 6918 | 7718 |
| Independent reflections | 4170 [R _{int} = 0.0958, R _{sigma} = 0.1323] | 4310 [R _{int} = 0.0362, R _{sigma} = 0.0583] |
| Data/restraints/parameters | 4170/0/246 | 4310/0/258 |
| Goodness-of-fit on F ² | 1.042 | 1.151 |
| Final R indexes [I >= 2σ (I)] | R ₁ = 0.0543, wR ₂ = 0.0990 | R ₁ = 0.0463, wR ₂ = 0.1031 |
| Final R indexes [all data] | R ₁ = 0.0890, wR ₂ = 0.1295 | R ₁ = 0.0518, wR ₂ = 0.1065 |
| Largest diff. peak/hole / e Å ⁻³ | 0.76/-1.71 | 1.38/-0.97 |

Table 2

Thermal decomposition data (in air flow) for complexes

| Complex | Step | Thermal effect | Temperature range/ °C | $\Delta m_{\text{exp}}/\%$ | $\Delta m_{\text{calc}}/\%$ |
|---|---------------|----------------|-----------------------|----------------------------|-----------------------------|
| [Zn(ac) ₂ (NA) ₂] (1) | 1 | Endothermic | 132 | – | – |
| | 2 | Endothermic | 155–320 | 57.7 | 57.1 |
| | 3 | Miscellaneous | 320–460 | 22.9 | 23.9 |
| | Residue (ZnO) | | | 19.4 | 19.0 |
| [Cd ₂ (ac) ₄ (NA) ₄].2H ₂ O (2) | 1 | Endothermic | 75–130 | 3.6 | 3.7 |
| | 2 | Endothermic | 162–295 | 50.4 | 49.5 |
| | 3 | Exothermic | 295–445 | 19.6 | 20.7 |
| | Residue (CdO) | | | 26.4 | 26.1 |

DISCUSSION

FT-IR spectra

The IR spectra of both complexes exhibit bands in the range 3450 – 3150 cm⁻¹ which were assigned to the asymmetric (complex **1**) – 3419 cm⁻¹ and complex **2**) – 3352 cm⁻¹) and symmetric (3291, 3210 cm⁻¹ – **1**); **2**) – 3176 cm⁻¹) N-H stretching vibrations of the amido group belonging to nicotinamide molecules.¹⁹ The splitting observed in the spectrum of complex **2**) for ν_s (N-H) band is probably due to the involvement of the nitrogen atom in two different types of hydrogen bondings. Additionally, in the spectrum of the Cd(II) complex, the shoulder from 3536 cm⁻¹, due to ν (O-H) vibration, shows the presence of the water molecules in its crystalline lattice. In the spectrum of Zn(II) complex, the bands specific to the asymmetric and symmetric valence vibrations of the acetate groups are situated at 1573 and 1382 cm⁻¹. In the complex **2**) spectrum, the same bands are observed at 1556 – ν_{as} (COO⁻), 1392 and 1385 cm⁻¹ – ν_s (COO⁻), the splitting being probably assignable to the two different coordination modes of the acetate groups. Anyway, the Δ value = $\nu_{\text{as}}(\text{COO}^-) - \nu_s(\text{COO}^-)$ is greater (191 cm⁻¹) for

complex **1**) than for complex **2**) (164 cm⁻¹), showing the difference between the monodentate and the chelating bidentate coordination modes.²⁰ The coordination of acetate groups to the central metal ion is sustained by the maxima situated around 430 cm⁻¹, due to the metal – oxygen valence vibrations.²¹

X-ray crystallography

The crystal structure of Zn-nicotinamide (C₁₆H₁₈N₄O₆Zn) was elucidated using single crystal X-ray diffraction analysis and it was shown that the complex crystallizes in the centrosymmetric P-1 space group. The asymmetric unit of the complex is comprised by one central metal Zn²⁺ ion, two acetate anions (CH₃COO⁻) and two nicotinamide molecules (Fig. 3a). The unit cell is comprised by two such asymmetric units generated by symmetry. The metal is four coordinated, the overall coordination environment being comprised by the two nicotinamide molecules which act as monodentate, being coordinated via N1 and N2 nitrogen atoms of the pyridine rings, and the two acetate oxygen atoms, O1 and O3. In Table 3, we present the values of some selected bond distances and angles.

Table 3

Selected bond distances (Å) and angles (°) for the complex **1**)

| Bond | Bond distance | Atoms | Angle |
|----------|---------------|---------------|-----------|
| Zn1 – O1 | 1.960(4) | O1 – Zn1 – O3 | 114.50(1) |
| Zn1 – O3 | 1.941(4) | O3 – Zn1 – N2 | 117.97(1) |
| Zn1 – N1 | 2.044(4) | O3 – Zn1 – N1 | 114.50(1) |
| Zn1 – N2 | 2.052(3) | O1 – Zn1 – N2 | 96.90(1) |

More precisely, the asymmetric unit depicts a distorted tetrahedral geometry with the

coordination angles O1-Zn-N2 of 96.90° being the smallest and O3-Zn-N2 angle of 117.97° the

highest angle value. The Zn-O_{acetate} distances, Zn-O1 and Zn-O3, are 1.960 Å and 1.941 Å respectively, meanwhile Zn-N_{pyridine} (Zn-N1 and Zn-N2 are 2.044 Å and 2.052 Å) are similar to other Zn complexes.^{22,23}

In the formation of supramolecular self-assemblies and solid state cohesion of the complex are included combinations of N-H...O hydrogen bonds, the geometries of hydrogen bonds being presented in Table 5. Both NH₂ amide groups are participating as donors in the formation of the hydrogen bonds with the oxygen acceptors of acetate and the carbonyl of one amide. In Fig. 3b is presented the formation of R₂²(8) heterosynthon by the use of mutual N3-H...O6 interactions for adjacent nicotinamide-nicotinamide molecules.

The Cd-nicotinamide complex (C₁₆H₂₀N₄O₇Cd) crystallizes triclinically in the centrosymmetric P-1 space group with the asymmetric unit consisting of

one metal ion (Cd²⁺), two acetate anions (CH₃COO⁻), two nicotinamide molecules and one lattice water molecule (Fig. 4a). The packing of the complex (2) in the unit cell is shown in Fig. 4b. It can be noted that through the inversion operation of the P-1 group, the asymmetric unit doubles. In the asymmetric unit, the metal is six-coordinated, so that both nicotinamide molecules participate in the coordination through the nitrogen of the pyridine rings (N1 and N2) in a similar way to complex (1). Also, each acetate anion participates in the coordination through the both oxygen atoms (O3, O4, O6, O7), one of the acetate anion acting in a bidentate chelate manner and the other in a bridging bidentate chelate manner. Overall, this depicts a pentagonal bipyramid geometry for each Cd(II) in the dimeric complex. Selected bond distances and angles for the complex (2) are presented in Table 4.

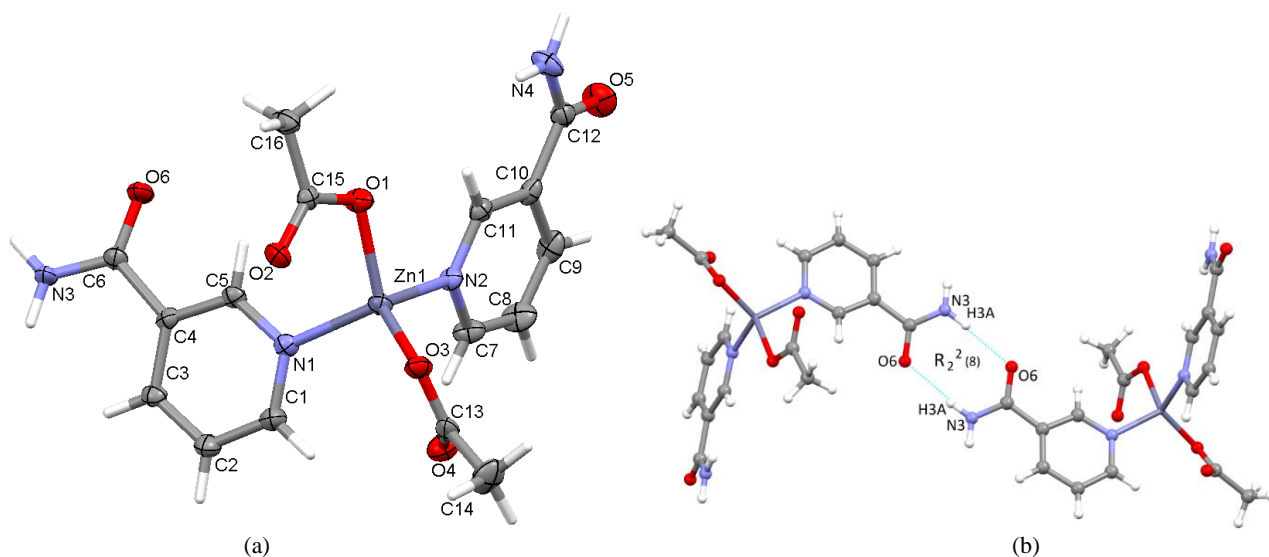


Fig. 3 – Asymmetric unit of (1) complex presenting non-hydrogen atoms at 50% probability level (a); Mutual N-H...O hydrogen bonds illustrating the formation of R₂²(8) motifs (b).

Table 4

Selected bond distances (Å) and angles (°) for the complex (2)

| Bond | Bond distance | Atoms | Angle |
|----------|---------------|---------------|----------|
| Cd1 – O3 | 2.421(3) | O6 – Cd1 – O7 | 53.9(1) |
| Cd1 – O6 | 2.368(3) | O3 – Cd1 – O4 | 54.9(1) |
| Cd1 – O4 | 2.362(3) | O3 – Cd1 – O6 | 163.2(1) |
| Cd1 – O7 | 2.460(3) | O7 – Cd1 – O4 | 87.8(1) |
| Cd1 – N1 | 2.327(4) | O6 – Cd1 – N2 | 88.0(1) |
| Cd1 – N2 | 2.335(3) | O6 – Cd1 – N1 | 93.0(1) |

The values of the coordination angles are situated between 53.9° for O6-Cd-O7 and the highest value of

163.2° for O3-Cd-O6. The coordination distances of the metal atom are Cd-N_{pyridine} (Cd-N1 of 2.327 Å and

Cd-N2 of 2.335 Å) while the Cd-O_{acetate} distances are 2.421 Å for Cd-O3, 2.362 Å for Cd-O4, 2.368 Å for Cd-O6 and 2.460 Å for Cd-O7. For the oxygen atoms which act as bridge, the Cd-O lengths are 2.349 Å and 2.368 Å respectively. Similar coordination distances have been reported in other cadmium complexes.^{24, 25} The structural difference between this compound and the previously reported one¹⁸ is given by the two lattice water molecules.

Overall crystal cohesion is assured by a multitude of N-H...O, O-H...O and C-H...O

hydrogen bonds with the primary amides (NH₂), water molecules, methyl group of acetate and C-H groups of pyridine rings serving as donors while the acetate ions and amide groups as acceptors (Table 5). The embedded water molecules within the lattice are serving as hydrogen bond bridges, interconnecting the acetate ions with amide groups of the complex. A remark worth mentioning is the existence of $\pi \cdots \pi$ interactions between the pyridine rings, with a separation distance of 3.357 Å (Fig. 4c).

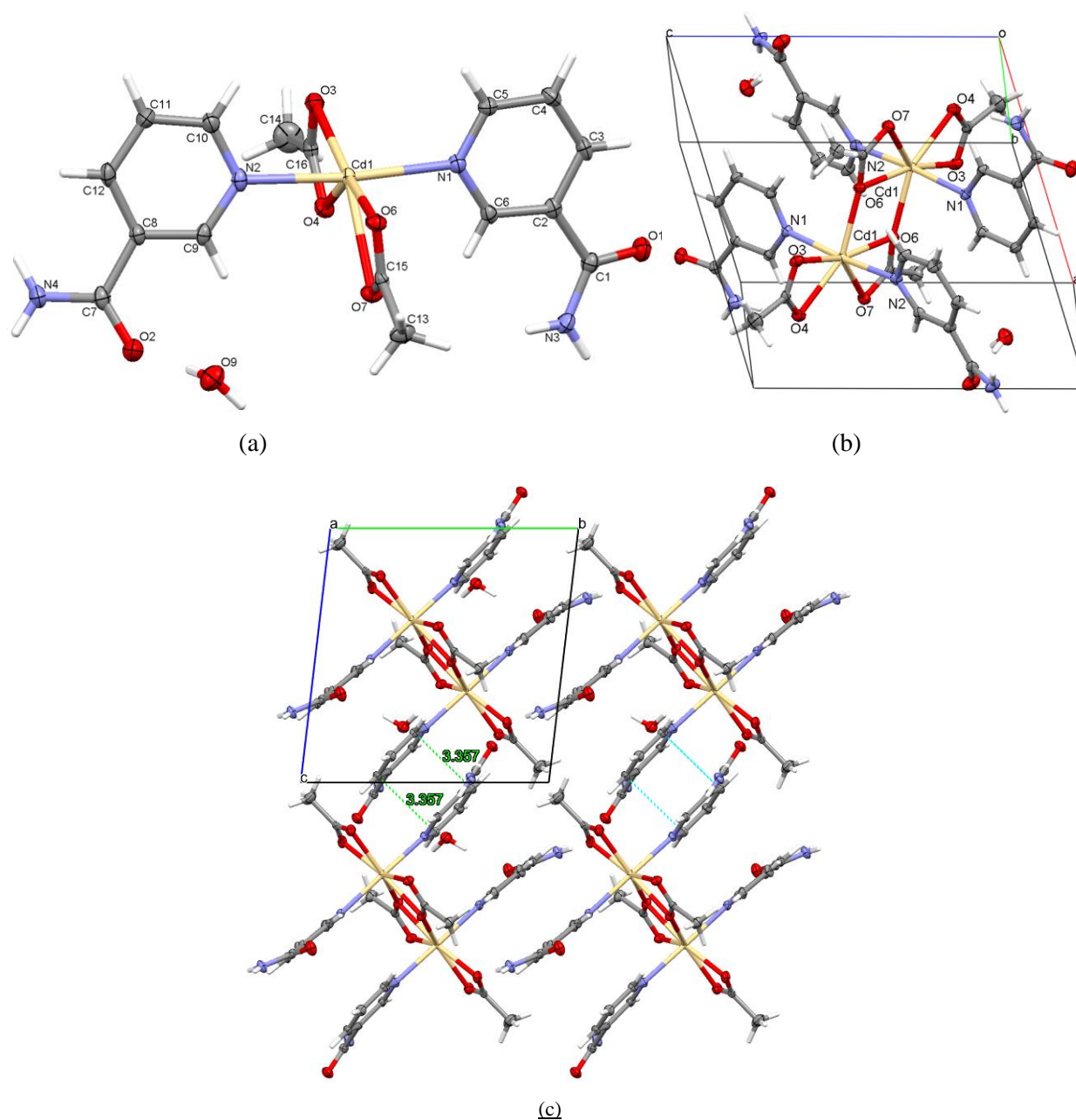


Fig. 4 – Asymmetric unit of (2) complex presenting non-hydrogen atoms at 50% probability level (a); unit cell packing (b); overall crystal packing along a-axis (c).

Table 5
Hydrogen bonds geometry for (1) and (2) complexes (Å, °)

| (1) | D-H...A | D-H | H...A | D...A | <(D-H...A) |
|-----|--|-------|----------|----------|------------|
| | N3-H3A...O6 ⁽ⁱ⁾ _(amide) | 0.860 | 2.049(3) | 2.924(4) | 172.6(1) |
| | N4-H4A...O6 ⁽ⁱⁱ⁾ _(amide) | 0.860 | 2.127(2) | 2.905(5) | 147.0(1) |
| | N3-H3B...O2 ⁽ⁱⁱⁱ⁾ _(acetate) | 0.860 | 1.920(1) | 2.789(2) | 169.1(8) |
| | N4-H4B...O3 ^(iv) _(acetate) | 0.860 | 2.062(4) | 2.880(5) | 154.3(3) |
| (2) | O9-H9A...O2 ^(v) _(amide) | 0.849 | 1.990(1) | 2.838(3) | 176.1(5) |
| | O9-H9B...O7 ^(vi) _(amide) | 0.850 | 2.016(2) | 2.862(3) | 173.3(5) |
| | N3-H3B...O9 ^(vi) _(water) | 0.860 | 2.154(3) | 2.954(2) | 154.6(8) |
| | N4-H4B...O1 ^(vii) _(amide) | 0.860 | 2.066(3) | 2.826(4) | 147.0(2) |
| | N4-H4A...O4 ^(viii) _(acetate) | 0.860 | 2.086(4) | 2.891(1) | 155.5(5) |
| | C11-H11...O3 ^(ix) _(acetate) | 0.930 | 2.584(4) | 3.235(3) | 127.4(4) |
| | C3-H3...O3 ⁽ⁱⁱⁱ⁾ _(acetate) | 0.930 | 2.505(4) | 3.354(2) | 152.0(1) |
| | C13-H13B...O7 ^(vi) _(acetate) | 0.960 | 2.540(1) | 3.449(3) | 178.2(8) |
| | C13-H13C...O1 ^(x) _(amide) | 0.960 | 2.545(3) | 3.243(3) | 129.6(5) |
| | C13-H13A...O2 ^(vi) _(amide) | 0.960 | 2.519(4) | 3.438(5) | 160.2(6) |
| | C12-H12...O1 ^(vii) _(amide) | 0.930 | 2.702(1) | 3.582(3) | 158.1(1) |

Symmetry code: (i) 2-x, 1-y, 2-z; (ii) 1-x, -y, 1-z; (iii) 1-x, 1-y, 2-z; (iv) -x, -y, 1-z; (v) x, y, z; (vi) 2-x, 1-y, 1-z; (vii) x, 1+y, -1+z; (viii) 2-x, 2-y, 1-z; (ix) 1-x, 2-y, 1-z; (x) 1-x, 1-y, 2-z; (vi) 2-x, 1-y, 1-z; (x) x, y, -1+z; (k-b) 2-x, 1-y, 1-z;

Thermal behavior

The thermal analysis method is commonly used to gather valuable insights into both the composition and stability of complexes. Consequently, the thermal behaviour of complexes was studied in air through simultaneous TG/DSC analysis. The thermal decomposition data are summarized in Table 2 and will be further discussed.

Figure 5 displays the TG and DSC curves recorded for Zn complex (1), illustrating that this compound is anhydrous and does not decompose up to 155 °C. The DSC curve indicates that it melts at 132 °C. Complex (1) undergoes a two-

step decomposition in the temperature range of 155–460 °C. Based on the TG curve, the first step corresponds to nicotinamide release while the second one is consistent with oxidative degradation of acetate anion. The final residue is zinc oxide.

For complex (2), the thermogravimetric analysis (Fig. 6) shows a weight loss in the range 75–130 °C, corresponding to the elimination of two water molecules. The low temperature range associated with this process confirm the presence of lattice water, first evidenced by X-ray crystallography. After water release, the thermal decomposition is quite similar with zinc complex, the final residue being CdO.

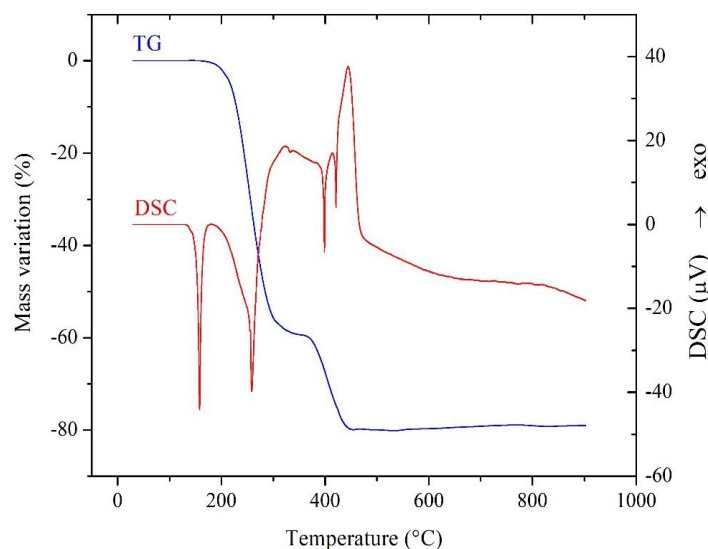


Fig. 5 – TG and DSC curves for the compound [Zn(ac)₂(NA)₂].

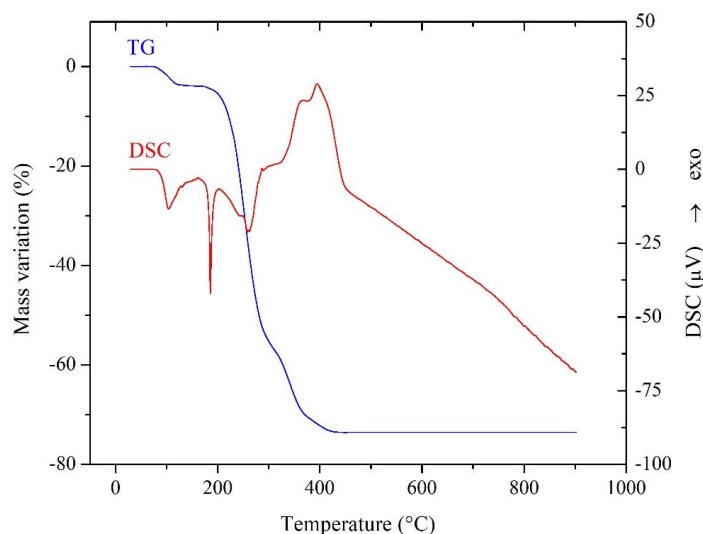


Fig. 6 – TG and DSC curves for the compound $[\text{Cd}_2(\text{ac})_4(\text{NA})_4] \cdot 2\text{H}_2\text{O}$.

EXPERIMENTAL

Materials

The chemicals for the synthesis of the complexes were purchased from Sigma-Aldrich (Darmstadt, Germany) as reagent grade and were used as received, without further purification.

Synthesis of the complex $[\text{Zn}(\text{ac})_2(\text{NA})_2]$

To an ethanolic solution of zinc acetate dihydrate (0.219 g, 1 mmol) in 10 mL ethanol was added an ethanolic solution (10 mL) of nicotinamide (0.244 g, 2 mmol). The mixture was magnetically stirred for 30 min. at room temperature and then it was refluxed for 1 h. After cooling and filtration, the solution was left at room temperature for slow evaporation. In a few days, white crystals, suitable for X-ray diffraction, were separated. Analysis found: C, 44.4; H, 4.27; N, 13.5%; calculated for $\text{ZnC}_{16}\text{H}_{18}\text{N}_4\text{O}_6$ ($M_w = 427.71$): C, 44.89; H, 4.20; N, 13.09 %.

Synthesis of the complex $[\text{Cd}_2(\text{ac})_4(\text{NA})_4] \cdot 2\text{H}_2\text{O}$

Cadmium acetate dihydrate (0.266 g, 1 mmol) was dissolved in 10 mL ethanol and was mixed with 10 mL of ethanolic solution of nicotinamide (0.244 g, 2 mmol). The mixture was stirred for 15 min. at room temperature and then was refluxed for 2 h. After cooling and filtration, the solution was left at room temperature for slow evaporation. In several days, white crystals suitable for X-ray diffraction were separated. Analysis found: C, 38.50; H, 4.18; N, 11.10 %; calculated for $\text{CdC}_{16}\text{H}_{20}\text{N}_4\text{O}_7$ ($M_w = 492.76$): C, 38.96; H, 4.06; N, 11.36 %.

Elemental analysis. A FlashSmart Thermo Fisher Scientific elemental analyzer was used for chemical analyses (C, H, and N).

FT-IR. Fourier Transformed Infrared Spectroscopy spectra were recorded with JASCO 4200 FT-IR spectrometer covering field $400 - 4000 \text{ cm}^{-1}$.

Thermogravimetric analysis. The heating curves (TG and DSC) were recorded using a Themys one SETARAM instrument. The measurements were carried out in synthetic air, with a heating rate of 10 K min^{-1} .

X-ray single crystal diffraction and refinement.

Suitable plate-like single crystals of complexes were attached on a nylon loop and mounted on the goniometer of a SuperNova diffractometer which is equipped with dual radiation micro-sources (Cu and Mo), Eos CCD detector, X-ray tube operating at 50 kV and 0.8 mA. Data collection, correction of Lorentz, polarization and absorption effects was carried in CrysAlis PRO.²⁶ The crystal structures were solved with SHELXT program²⁷ using Intrinsic Phasing and refined via SHELXL²⁸ refinement package by Least Squares minimization in Olex2 software.²⁹ Carbon bound hydrogen atoms were located and treated by riding procedure, considering the isotropic displacement parameter $\text{Uiso}(\text{H})=1.2\text{Ueq}(\text{C})$ for ternary CH groups [$\text{C}-\text{H}=0.93 \text{ \AA}$] and $1.5\text{Ueq}(\text{C})$ considered for all methyl CH_3 groups [$\text{C}-\text{H}=0.96 \text{ \AA}$]. Nitrogen bound hydrogen atoms were treated and refined as riding [$\text{N}-\text{H}=0.86 \text{ \AA}$]. Oxygen bound hydrogen atoms were treated as riding as well, with [$\text{O}-\text{H}=0.85 \text{ \AA}$] for the water molecule and [$\text{O}-\text{H}=0.82 \text{ \AA}$] for hydroxyl groups.

NMR spectra. The NMR spectra were recorded on a Bruker Avance III Ultrashield Plus 500 MHz spectrometer, operating at 11.74 T, corresponding to the resonance frequency of 500.13 MHz for the ^1H nucleus, equipped with a direct detection four nuclei probe head and field gradients on z axis.

CONCLUSIONS

In this work, we describe the synthesis and the characterization of two new complexes of Zn(II) and Cd(II) with acetate and nicotinamide as mixed ligands. Both compounds were obtained starting from the acetates of the metals. The Zn(II) complex is mononuclear, while the Cd(II) complex is binuclear, with the acetate groups coordinated in two ways: bidentate chelate and bridging bidentate chelate. The nicotinamide molecules are

coordinated through the pyridinic nitrogen. The geometry of Zn(II) is distorted tetrahedral, while the Cd(II) geometry is distorted pentagonal bipyramid. Both complexes were characterized by means of single-crystal X-ray diffraction, FT-IR, ¹H NMR and ¹³C NMR spectroscopy, elemental and thermal analysis.

Supplementary materials. CCDC deposition numbers 2302386 for **1** and 2302400 for **2** contains the supplementary crystallographic data for this paper. These data can be obtained free of charge via <http://www.ccdc.cam.ac.uk/conts/retrieving.html> (or from the Cambridge Crystallographic Data Centre, 12, Union Road, Cambridge CB2 1EZ, UK; fax: +44 1223 336033).

Acknowledgements. The service for the Oxford SuperNova diffractometer was supported by the Ministry of Research, Innovation, and Digitization through Programme 1-Development of the National Research and Development System, Subprogramme 1.2-Institutional Performance-Funding Projects for Excellence in RDI, Contract No. 37PFE/30.12.2021

REFERENCES

1. D. Keilin and T. Mann, *Biochem. J.*, **1940**, *34*, 1163–1176, DOI: 10.1042/bj0341163.
2. J. E. Coleman, *Curr. Opin. Chem. Biol.*, **1998**, *2*, 222–234, DOI: 10.1016/s1367-5931(98)80064-1.
3. Y. Yoshikawa and H. Yasui, *Curr. Top Med. Chem.*, **2012**, *12*, 210–218, DOI: 10.2174/156802612799078874.
4. C. I. Chukwuma, S. S. Mashele, K. C. Eze, G. R. Matowane, S. M. Islam, S. L. Bonnet, A. E. M. Noreljaleel and L. M. Ramorobi, *Pharmacol Res.*, **2020**, *155*, 104744, DOI: 10.1016/j.phrs.2020.104744.
5. V. R. Martínez, M. V. Aguirre, J. S. Todaro, A. M. Lima, N. Stergiopoulos, E. G. Ferrer and P. A. Williams, *Future Med. Chem.*, **2021**, *13*, 13–23, DOI: 10.4155/fmc-2020-0093.
6. E. Halevas, B. Mavroidi, M. Pelecanou and A. G. Hatzidimitriou, *Inorg. Chim. Acta*, **2021**, *523*, 120407, <https://doi.org/10.1016/j.ica.2021.120407>.
7. M. Abendrot, L. Checinska, J. Kusz, K. Lisowska, K. Zawadzka, A. Felczak and U. Kalinowska-Lis., *Molecules* **2020**, *25*, 951, DOI: 10.3390/molecules25040951.
8. R. M. Joseyphus and M. S. Nair, *Mycobiology*, **2008**, *36*, 93–98, DOI: 10.4489/MYCO.2008.36.2.093.
9. K. Aoshima, *Soil Sci. Plant Nutr.*, **2016**, *62*, 319–326, DOI:10.1080/00380768.2016.1159116.
10. T. Kondori, N. Akbarzadeh-T, K. Abdi, M. Dusek and V. Eigner, *J. Biomol. Struct. Dynam.*, **2020**, *38*, 236–247, DOI: 10.1080/07391102.2019.1570867.
11. S. Soltani, K. Akhbari and J. White, *Cryst. Eng. Comm.*, **2021**, *23*, 7450–7461, <https://doi.org/10.1039/D1CE00979F>.
12. L. Saghatforoush, V. Matarranz, F. Chalabian, S. Ghammamy, F. Katouzian, *J. Chem. Sci.*, **2012**, *124*, 577–585, <https://doi.org/10.1007/s12039-012-0246-0>.
13. F. A. Al-Saif and M. S. Refat, *J. Mol. Struct.*, **2012**, *1021*, 40–52, <https://doi.org/10.1016/j.molstruc.2012.04.057>.
14. K. Kralova, E. Masarovicova, J. Lesikova and I. Ondrejovicova, *Chem. Pap.*, **2006**, *60*, 149–153, <https://doi.org/10.2478/s11696-006-0027-7>.
15. A. Fargasova, A. Filova, I. Ondrejovičová, T. Mackurak, *Chem. Pap.*, **2018**, *72*, 2273–2281, <https://doi.org/10.1007/s11696-018-0488-5>.
16. B. Dojer, A. Pevec, F. Belaj and M. Kristl, *Acta Chim. Slov.*, **2015**, *62*, 312–318, <https://doi.org/10.17344/acsi.2014.1111>.
17. G. J. Brewer, *Expert Opin. Pharmacoter.* **2001**, *2*, 1473–1477, DOI: 10.1517/14656566.2.9.1473.
18. Z. Soldin, B.-M. Kukovec, M. Kovacic, M. Dakovic and Z. Popovic, *Chemistry*, **2023**, *5*, 1357–1368, <https://doi.org/10.3390/chemistry5020092>.
19. S. Ramalingam, S. Periandy, M. Govindarajan and S. Mohan, *Spectrochim. Acta A Mol. Biomol. Spectrosc.*, **2010**, *75*, 1552–1558, DOI: 10.1016/j.saa.2010.02.015.
20. K. Nakamoto, “Infrared and Raman spectra of inorganic and coordination compounds”, Part B – “Applications in coordination, organometallic, and bioinorganic chemistry”, 6th edition, John Wiley & Sons, Inc., 2009, pp. 231–233.
21. H.-R. Jia, J. Li, J.-Q. Guo, B. Yu, N. Wen and L. Xu, *Crystals*, **2017**, *7*, 247, <https://doi.org/10.3390/cryst7080247>.
22. J. A. do N. Neto, C. C. da Silva, L. Ribeiro, G. A. Vasconcelos, B. G. Vaz, V. S. Ferreira, L. H. K. Queiroz Junior, L. J. Q. Maia, A. M. Sarotti and F. T. Martins, *New J. Chem.*, **2017**, *41*, 12843–12853, doi:10.1039/C7NJ02393F.
23. P. Comba, M. Jakob, K. Ruck and W. Wadepohl, *Inorg. Chim. Acta*, **2017**, *481*, 98–105, doi:10.1016/j.ica.2017.08.022.
24. X. Wang, X. Shi, T. Yang, L. Hongwen and W. Lu, *J. Chem. Cryst.*, **2021**, *51*, 50–56, doi:10.1007/s10870-020-00825-6.
25. Y.-Q. Su, L. Fu and G.-H. Cui, *Dalton Trans.*, **2021**, *50*, 15743–15753, doi:10.1039/D1DT03205D.
26. CrysAlis PRO, Rigaku Oxford Diffraction, Yarnton, Oxfordshire, England, 2015.
27. G. M. Sheldrick, SHELXT – Integrated space-group and crystal-structure determination, *Acta Cryst.*, **2015**, *A71*, 3–8, <https://doi.org/10.1107/S2053273314026370>.
28. G. M. Sheldrick, *Acta Cryst.*, **2008**, *A64*, 112–122, <https://doi.org/10.1107/S0108767307043930>.
29. O. V. Dolomanov, L. J. Bourhis, R. J. Gildea, J. A. K. Howard and H. J. Puschmann, *Appl. Cryst.*, **2009**, *42*, 339–341, <https://doi.org/10.1107/S0021889808042726>.

